https://doi.org/10.5194/egusphere-2024-1523
Preprint. Discussion started: 27 May 2024

European forest cover during the Holocene reconstructed from pollen records

Luke Sweeney[1,2,*], Sandy P. Harrison[1,2], Marc Vander Linden[3]

1: Geography and Environmental Science, School of Archaeology, Geography and Environmental Science (SAGES), University of Reading, Whiteknights, Reading, RG6 6AH, UK. Email: l.sweeney@pgr.reading.ac.uk

2: Leverhulme Centre for Wildfires, Environment and Society, Imperial College London, South Kensington, London, SW7 2BW, UK. Email: s.p.harrison@reading.ac.uk

3: Institute for the Modelling of Socio-Environmental Transitions, Bournemouth University, Christchurch House, Talbot Campus, Poole, BH 12 5BB, UK. Email: mvanderlinden@bournemouth.ac.uk

Correspondence to: Luke Sweeney (l.sweeney@pgr.reading.ac.uk)

Abstract

Changes in tree cover influence many aspects of the Earth System. Recent regional changes in tree cover, as documented by remote-sensed observations, are insufficient to capture the response to large climate changes or to differentiate the impacts of human activities from natural drivers. Pollen records provide an opportunity to examine the causes of changes in tree cover in response to large climate changes in the past and during periods when human influence was less important than today. Here we reconstruct changes in tree cover in Europe through the Holocene using fossil pollen records, using the modelled relationship between observed modern tree cover and modern pollen samples. At a pan-European scale, tree cover is low at the beginning of the Holocene but increases rapidly during the early Holocene and is maximal at ca. 6,500 cal. BP, after which tree cover declines to present-day levels. The rapidity of the post-glacial increase in tree cover and the timing and length of maximum tree cover varies regionally, reflecting differences in climate trajectories during the early and mid-Holocene. The nature of the subsequent reduction in tree cover also varies, which may be due to differences in climate but may also reflect different degrees of human influence. The reconstructed patterns of change in tree cover are similar to those shown by previous reconstructions, but our approach is more robust and less data-demanding than previously applied methods and therefore provides a useful approach to reconstructing tree cover in regions where data limitations preclude the use of alternative methods.

https://doi.org/10.5194/egusphere-2024-1523
Preprint. Discussion started: 27 May 2024

1. Introduction

Forest cover in Europe has been expanding in recent decades (FAO, 2020; Turubanova et al., 2023), with potential implications for land-atmosphere energy exchanges, water and carbon cycles, and ultimately local and global climates (Bonan, 2008; Alkama and Cescatti, 2016). Tree cover both affects and is affected by the environment (Moyes et al., 2015; Abis and Brovkin, 2017) and this two-way relationship leads to complex interactions between both. For example, deforestation in the Amazon has been linked to changes in weather patterns, which subsequently affect the moisture available for rainforest maintenance (Staal et al., 2018; Leite-Filho et al., 2020). Similarly, increases in tree cover resulting from farm abandonment has been shown to change fire frequency in the Iberian Peninsula (Moreira et al., 2001; Viedma et al., 2015), which in turn affects vegetation cover and structure and results in further changes to the fire regime. Satellite data can be used to assess the environmental controls on tree cover but, since they only cover the past 20-30 years, are insufficient to look at the response to longer term changes in climate or relationships when the human influence of land-use and vegetation cover was less ubiquitous.

Pollen from sedimentary sequences provides a record of past vegetation changes. The relative abundance of arboreal pollen is commonly used to infer changes in tree abundance at a site. The relationship between pollen abundances and vegetation cover is not straightforward however, because it is influenced by differences between species in pollen productivity and transportability, and site characteristics that affect the pollen source area, such as basin size (Bradshaw and Webb, 1985; Prentice and Webb, 1986; Prentice, 1988; Sugita, 1993).

The most recent quantitative pan-European pollen-based reconstructions of Holocene vegetation changes have been made using the Landscape Reconstruction Algorithm (LRA) REVEALS approach (Sugita, 2007b, a) or the Modern Analogue Technique (MAT) (Overpeck et al., 1985; Guiot, 1990; Jackson and Williams, 2004). The REVEALS method calculates regional vegetation cover based on modelled relationships between pollen abundance, estimated differences in species level pollen productivity and pollen transport, and differences in site characteristics. Initially used at individual sites or small regions (e.g. Gaillard et al., 2010; Nielsen et al., 2012; Marquer et al., 2014), REVEALS was first applied at a pan-European scale by Trondman et al. (2015). They produced maps of plant functional types at record-containing 1º grid cells for five time periods during the Holocene, based on 636 sites and 25 pollen taxa. This pan-European analysis was extended by Githumbi et al. (2022), who applied REVEALS to more than 1100 pollen records across Europe using 31 taxa, and provided maps of landcover and species abundance at record-containing 1º grid cells in 500-year intervals before 700 cal. BP and for the subsequent intervals of 700-350 cal. BP, 350-100 cal. BP and 100 cal. BP- present. The most recent analysis by Serge et al. (2023), is based on 1607 records and tested the impact of including

https://doi.org/10.5194/egusphere-2024-1523
Preprint. Discussion started: 27 May 2024

additional taxa (n=46) on the vegetation reconstructions. In contrast, the MAT approach reconstructs past vegetation based on identifying modern analogues of fossil pollen assemblages, on the assumption that samples found in the fossil record that share a similar composition to those found in present-day pollen assemblages will have similar vegetation. Zanon et al. (2018) applied MAT to 2,526 individual fossil pollen samples from Europe to generate interpolated maps at 250-year intervals at 5 arc-minute resolution through the Holocene.

Each of these approaches presents challenges. The REVEALS approach is data demanding as it requires, and is sensitive to, estimates of relative pollen productivity (RPP) and pollen fall speeds (FS) for individual species (Bunting and Farrell, 2022; Githumbi et al., 2022; Serge et al., 2023). For instance, landscape-level reconstructions are problematic if RPP and FS information is not available for relatively common taxa. The MAT technique is less data demanding, although it requires a large modern pollen data set for training purposes, but involves a number of arbitrary decisions including the choice of analogue threshold (i.e. how similar modern and fossil assemblages must be to be considered analogous), and the number of analogues used (Jackson and Williams, 2004). Techniques designed to minimise the number of samples for which no analogues are found, such as grouping species into plant functional types (PFTs), introduce further uncertainties since the allocation of pollen taxa to PFTs is often ambiguous (Zanon et al., 2018).

In this paper, we develop a simple calibration approach to derive estimates of forest cover at individual sites across Europe, capitalising on an extensive modern pollen data set, new remote-sensed data on tree cover, and harmonised age models and improved information about basin size for fossil records from Europe. We evaluate how well this method reconstructs modern tree cover compared to existing methods. We then reconstruct pan-European changes in tree cover through the Holocene and compare these reconstructions with existing reconstructions.

2. Methods

Tree cover during the Holocene was reconstructed by applying a statistical model describing modern tree cover to fossil pollen records from individual sites. There were three steps: 1) selection and treatment of data; 2) development of the predictive model relating modern pollen data to modern tree cover; and 3) application of this model to fossil pollen records (Fig. 1). All analyses were performed using the R Statistical Software (R Core Team, 2022).

https://doi.org/10.5194/egusphere-2024-1523
Preprint. Discussion started: 27 May 2024

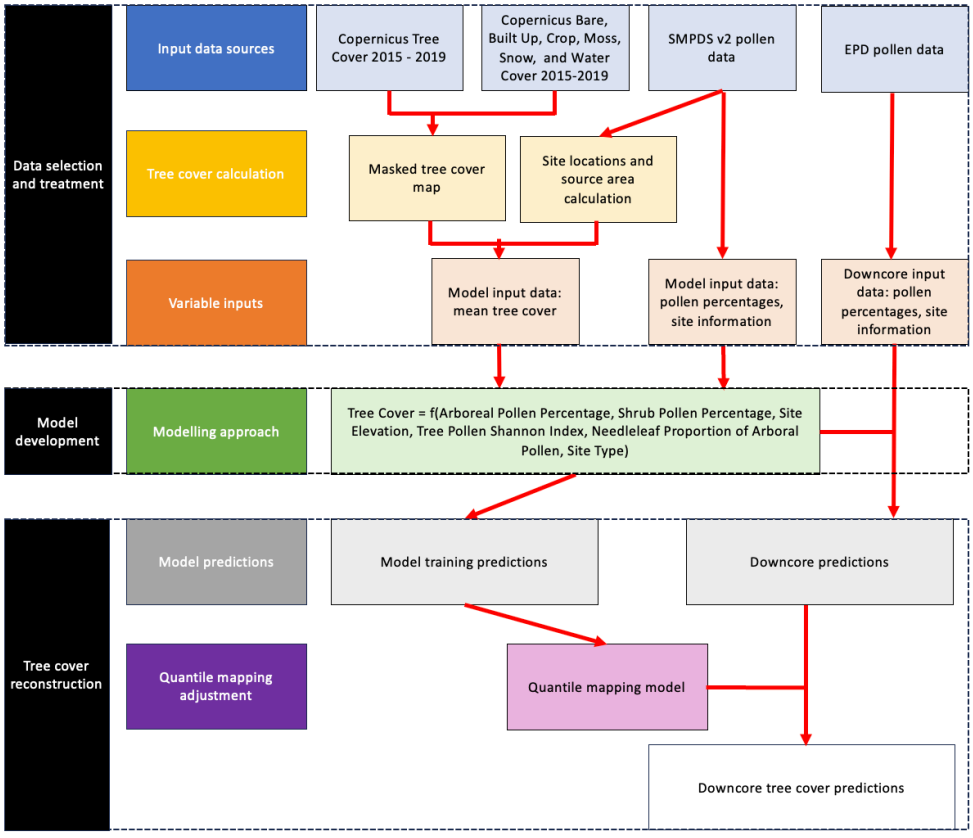

Figure 1: Methodology to reconstruct European tree cover during the Holocene

2.1 Selection and treatment of data

A composite map of modern tree cover for the region 12°W to 45°E and 34-73°N was generated by averaging annual percentage tree cover data from Copernicus annual land cover maps from 2015 to 2019 (Buchhorn et al., 2020a, e, d, c, b), after removing cells dominated (> 50%) by non-natural vegetation classes, including bare ground, built up areas, moss or lichen, permanent water, snow, and crops (Fig. 2A). This modern tree cover map has a resolution of 100m.

https://doi.org/10.5194/egusphere-2024-1523
Preprint. Discussion started: 27 May 2024

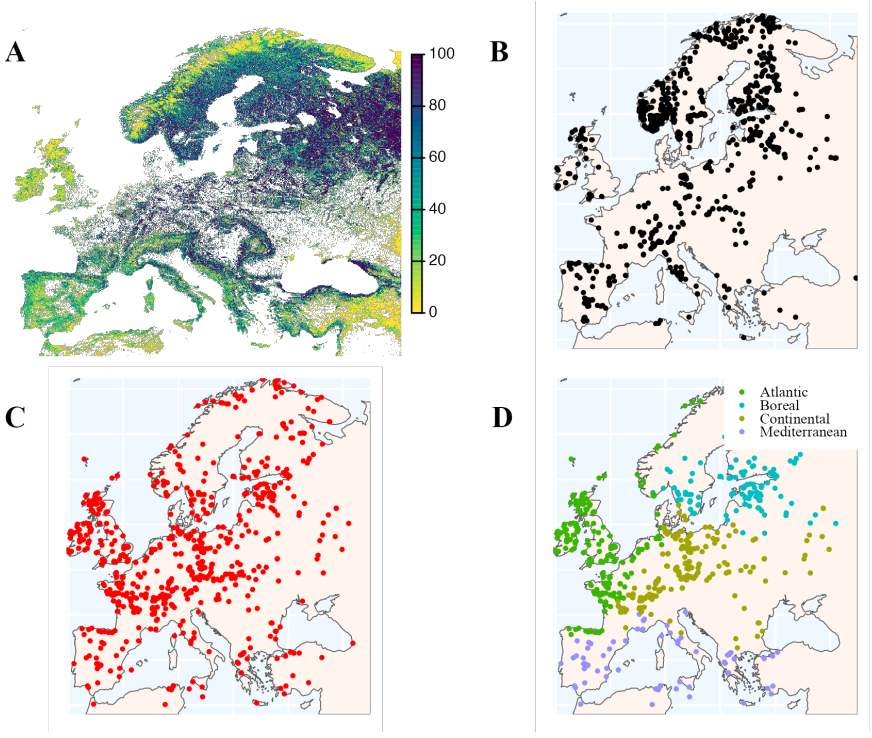

Figure 2: A - Observed tree cover based on compositing annual tree cover maps from the Copernicus land cover data sets (2015-2019) and screening out cells where the dominant land cover was not natural; B - Modern pollen records used for model fitting; C - Fossil pollen sites used for tree cover reconstructions; D - Classification of the fossil pollen sites into climatic sub-regions

Modern pollen data (Fig. 2B) was obtained from version 2 of the SPECIAL Modern Pollen Dataset (Villegas-Diaz and Harrison, 2022), amended to include updated meta information (see *Code and data availability*). The SMPDS contains pollen samples from the post-industrial era (post-1850 CE). We extracted samples that were explicitly dated to post-1950 and assumed that all samples characterised as modern but without an explicit age assignment also dated to post-1950 CE. We assume that at the regional scale these samples broadly reflect modern (2015-2019) tree cover values. Site metadata (elevation, site type, basin size) from the SMPDSv2, along with the additional metadata updates, were used as explanatory variables in the tree cover model (see below). Depauperate samples with Hill's N2 values (Hill, 1973) of < 2 were excluded, following Wei et al. (2021). Pollen counts from cores with multiple modern samples were averaged to prevent over-sampling. Likewise, where there were multiple cores from the same site, pollen counts were averaged so that there was only a single count from each site. Only samples from lakes and bogs were included, to ensure appropriate pollen source areas could be calculated. However, bog records with a radius $\geq$ 400m were excluded from the analysis, following Githumbi et al. (2022), because vegetation growing on the surface of large bogs can bias regional vegetation reconstructions. Finally, since upslope pollen transport is known to increase the proportion of non-local pollen at high-elevation sites (Fall, 1992; Ortu et al., 2008, 2010), and the complex

https://doi.org/10.5194/egusphere-2024-1523
Preprint. Discussion started: 27 May 2024

topography of mountainous areas also impacts pollen transport (Markgraf, 1980; Bunting et al., 2008; Wörl et al., 2022), we excluded 236 site records above 1000m. To test the effect of the inclusion of bog sites and the restriction on site elevation, we ran two alternative models excluding bogs and including high elevation sites, and examined summary statistics for each.

The percentage of arboreal pollen (AP%) and shrub pollen (SP%) were calculated based on the Total Terrestrial Pollen Sum (TTPS), and allocation of species into AP/SP or herbaceous (e.g. grass/ herb) pollen types in Europe (see Supplementary Information: S1 and *Code and data availability*). The pollen data were also used to calculate both the needleleaf share of the AP (%needleleaf), and the Shannon Index (SI) of tree species diversity. Species identified as not native to Europe, obligate aquatics and cereals were excluded from the TTPS, but Cyperaceae, Polypodiales and Ericaceae were included as characteristic of more open environments and to prevent the pollen assemblages from these environments being dominated by pollen transported from long distances.

The source area for each record, and hence the appropriate area for the calculation of mean tree cover, was calculated using Prentice's (1985) source area formula for 70% of pollen, and lake or bog area from the SMPDS. The original source area formula used species-specific FS values, but here we use the median FS (0.03) from Githumbi et al. (2022) and Serge et al. (2023) since the tree cover map represents the broad species community around each record location. We assumed basin areas were circular to calculate the radius. For those sites that have no exact information on basin size but were categorised as small (0.1-1km^2), we assumed basin areas of 0.5km^2: there were 30 such sites included in the model construction. Mean tree cover was calculated for each site from the tree cover map using the R package *exactextractr (*function*: exact_extract)* (Baston, 2023). There were 263 records where more than half of the contributing grid cells were masked as being non-natural vegetation; these were excluded from the model construction. A total of 852 pollen records were included in the final model training dataset.

Fossil pollen data were obtained from the SPECIAL-EPD dataset (Harrison et al., 2024), which includes 1,758 records from 1573 sites with Bayesian age-depth models made using the INTCAL20 Northern Hemisphere (Reimer et al., 2020) or Marine20 (Heaton et al., 2020) calibration curves as appropriate. We filtered the fossil data in the same way as the modern pollen data, by only using pollen records from lakes and bogs below 1000m in the region 12°W to 45°E and 34-73°N. Where there were multiple records from the same site, we selected a single record, prioritising the record with the maximum number of samples for the period 12,000 cal. BP to present (Fig. 2C). The pollen counts were used to calculate AP% and SP%, %needleleaf, and the tree SI, using the species categorisation applied to the modern pollen data (see Supplementary Information: S1 and *Code and data availability*).

https://doi.org/10.5194/egusphere-2024-1523
Preprint. Discussion started: 27 May 2024

2.2 Model development

A Beta regression, which is suitable for use with proportional data, was used to model tree cover using the R package *betareg* (Cribari-Neto and Zeileis, 2010). The explanatory variables included AP%, SP%, %needleleaf, site elevation, site type (lake or bog) and arboreal pollen SI values. The AP% and SP% are expected to explain most of the variability in tree cover, but %needleleaf was also included to reflect potential broad differences in pollen productivity and transport between needleleaf and broadleaf species (see Table 1 from Serge et al., 2023). Although records above 1000m were excluded from the data set, site elevation was included as an explanatory variable to capture any residual impacts of elevation on tree cover. Site type (bog, lake) was included because there is a greater potential for pollen mixing prior to sedimentation in lake settings, which means that lakes may be more representative of the regional tree cover (Sugita, 1993; Githumbi et al., 2022). SI was included because species diversity may reflect a more stable (Jactel et al., 2017) or less fragmented landscape (Hill and Curran, 2003). The final model was selected based on the Akaike Information Criteria (AIC: Akaike, 1974) and Cox-Snell R^2 value (Cox and Snell, 1989). We tested the inclusion of interaction effects associated with elevation, since the relationship between AP% and tree cover may be directly influenced by elevation due to upslope transport. In addition, given the potential importance of RPP and transport, and landscape fragmentation, we tested the inclusion of second and third order polynomial coefficients for %needleleaf and SI. Finally, as Beta regression allows explicit modelling of the precision parameter as well as the mean (i.e. variance does not need to be consistent across observations) (see Simas et al., 2010), we tested the inclusion of regressors describing precision.

The modern tree cover model was tested based on leave one out cross validation (LOOCV), and calculation of root mean squared error (RMSE), mean absolute error (MAE) and R^2 correlation between observed and predicted values. A quantile mapping adjustment, using the R package *qmap* (Gudmundsson et al., 2012) was calculated on the LOOCV model predictions to account for compression of the reconstructions, with overestimation of low tree cover and underestimation of high tree cover values, following Zanon et al. (2018). This decompression was then used to adjust downcore reconstructions generated from the Beta regression.

The final predictions were compared to modern reconstructions of tree cover by Serge et al. (2023) and Zanon et al. (2018), where modern is the interval 100 cal. BP and the present day in Serge et al. (2023) and between 125 cal. BP and present for Zanon et al. (2018). We make comparisons to the Serge et al. (2023) reconstructions based on the 31 taxa originally used by Githumbi et al. (2022) since they indicate that this produces better results than using the expanded data set of 46 taxa.

For each of the 1° grid cells in Serge et al. (2023), tree cover was calculated from the sum of the appropriate vegetation types. Time series of the change in median tree cover were constructed using

https://doi.org/10.5194/egusphere-2024-1523
Preprint. Discussion started: 27 May 2024

median tree cover corresponding to the pollen source area of each of our individual modern reconstructions. The tree cover time series for the Zanon et al. (2018) and Serge et al. (2023) data were initially constructed using the single grid cell values provided. However, since there are multiple sites used in our reconstruction in some of these grid cells, we tested whether this could affect the comparisons by attributing the appropriate grid cell values from Zanon et al. (2018) or from Serge et al. (2023) to each of the sites and then creating new time series for these two reconstructions.

2.3 Application of model to fossil pollen data

The tree cover model, adjusted to deal with the compression bias, was applied to the variables generated from 811 records from the SPECIAL-EPD with data for part or all of the interval between 12,000 cal. BP and the present day. Since the records cover different time periods and have different temporal resolutions, reconstructed tree cover values were binned in 200-year bins. We examined temporal trends in tree cover for the European region as a whole and for modern biogeographical regions as defined by the European Environment Agency (EEA) classification (European Environment Agency, 2016). We also produced maps of tree cover through time for 50km^2 grid cells by averaging reconstructed tree cover across all sites in the same cell. These reconstructions were compared with the Serge et al. (2023) and Zanon et al. (2018) reconstructions of Holocene tree cover. As basin size was not available for all record site locations, we extracted tree cover median values using a general 5 km^2 buffer to maximise the number of site comparisons and to prevent edge effects.

3. Results

3.1 Model fit and validation

The final model has a (Cox-Snell) pseudo-R^2 of 0.60, and LOOCV RMSE of 0.14 and a MAE of 0.11, indicating a reasonable fit to the data. Variance inflation factor (VIF) scores are not readily interpretable because of the inclusion of interaction terms, but a version of the model with the same variables but excluding the interaction terms has VIF values < 2 for all the explanatory variables, indicating that there is no multicollinearity and that all the explanatory variables represent independent controls on tree cover. The Cox-Snell R^2 for this final model is 0.54.

There is a positive relationship between tree cover and AP% and a negative relationship between tree cover and SP% (Table 1), as expected. However, the strength of each relationship is moderated by elevation, with increasing elevation reducing both the positive effect of AP% and the negative effect of SP% on tree cover. There is a negative correlation between %needleleaf and tree cover, although the significant positive quadratic term for needleleaf suggests this relationship becomes positive at higher

https://doi.org/10.5194/egusphere-2024-1523
Preprint. Discussion started: 27 May 2024

abundances of %needleleaf. Increased SI is positively related to tree cover, with the effect decreasing with elevation. However, the negative correlation for the quadratic term for the SI suggests that the relationship has less of an effect on tree cover as SI increases. There is no significant relationship between site type and tree cover, but the interaction term between them is significant, with a reduction in the effect of elevation on the likelihood of higher tree cover for lake sites. One possible explanation for this relationship is that the increasing likelihood of longer distance pollen transport with elevation affects bog sites more than lake sites in a relative sense, in that bog sites typically have a smaller source area. The Cox-Snell R^2 value increases slightly to 0.62 (from 0.60) if bogs are excluded from the model (Supplementary Information: S2) but this causes a substantial reduction in spatial and temporal coverage. Conversely, including higher elevation sites (>1000 m) within the model reduces the Cox-Snell R^2 to 0.50 (from 0.60) (Supplementary Information: S3). A likelihood-ratio test of the model with the inclusion of variables for precision against a model with a constant precision parameter shows that there is a significant improvement in the model with variable dispersion. Increases in %needleleaf and SI are associated with increased precision of the tree cover reconstructions, whereas lake sites are generally less variable in terms of tree cover than bog sites.

Table 1: Modern tree cover model coefficients

Coefficients (mean model with logit link)	**Estimate**	**Standard Error**	**P Value**
(Intercept)	-5.598	0.437	1.54e-37 ***
Tree pollen %	2.374	0.223	1.56e-26 ***
Shrub pollen %	-3.458	0.630	4.06e-08 ***
Needle share of AP%	-1.317	0.456	0.004 **
Needle share of AP%^2	3.009	0.514	4.80e-09 ***
AP Shannon index	5.091	0.458	1.04e-28 ***
AP Shannon index^2	-1.375	0.138	2.09e-23 ***
Lake or bog site	0.031	0.132	0.815
Elevation	0.003	0.001	0.005 **
AP pollen:elevation interaction	-0.001	0.000	0.003 **
SP pollen:elevation interaction	0.004	0.001	0.001 **
AP Shannon:elevation interaction	-0.004	0.001	2.06e-04 ***
AP Shannon^2:elevation interaction	0.002	0.000	2.10e-06 ***
Lake or bog site:elevation interaction	-0.001	0.000	5.57e-04 ***
Precision submodel (log link; after variable selection^)			
(Intercept)	0.407	0.256	0.112
Needle share of AP%	0.798	0.229	5.05e-4 ***

https://doi.org/10.5194/egusphere-2024-1523
Preprint. Discussion started: 27 May 2024

AP Shannon index	0.840	0.121	4.04e-12 ***
Lake or bog site	0.534	0.126	2.17e-5 ***

Significance codes: 0 = '***'; 0.001 = '**'; 0.01 = '*'; 0.05 = .' 0.1; ' ' = 1

^Only significant (at 5% significance) covariates were included

The application of the quantile mapping approach reduced the bias towards the mean, whilst preserving the general structure of the data (Supplementary Information: S4). However, there is still a tendency for under- and over-estimation at low and high observed tree cover respectively in the final model (Fig. 3A). There is no obvious spatial patterning in the biases, except for a tendency to overestimate tree cover in northernmost Scandinavia (Supplementary Information: S5). The correlation between the final "decompressed" predictions and observed tree cover values is 0.80 (Fig. 3B).

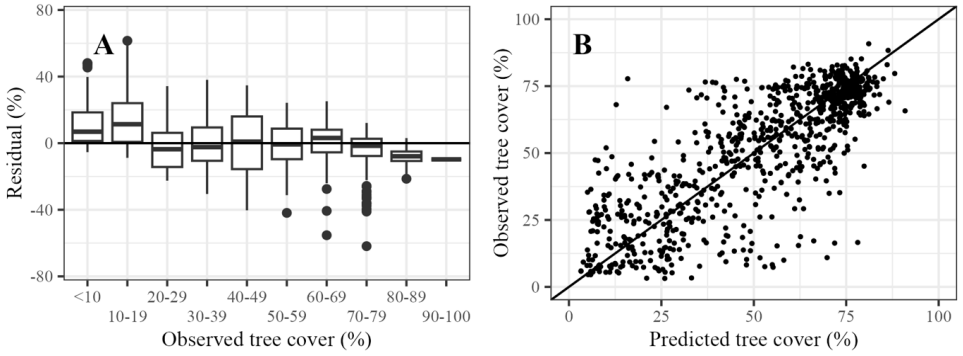

Figure 3: Evaluation of final model performance. A – Differences between predictions and observations (residual), in bins of observed tree cover percentage; B – Predictions of tree cover compared to observed tree cover

Our modern predictions differ from those of Serge et al (2023) and Zanon et al. (2018) (Figure 4). The correlation between the Zanon et al. (2018) reconstructions and observed tree cover is 0.78, which is similar to the correlation between our predictions and observed tree cover (0.8). The Zanon et al (2018) reconstructions have fewer outliers, but nevertheless they underestimate tree cover at high levels of observed tree cover (Figure 4A). The correlation between the Serge et al. (2023) predictions and observations is only 0.5. This is partly caused by the use of larger 1º grid cells, but even when taking this into account and comparing with an average value for each grid cell, the correlations between predictions and observations were still lower (0.59) than our predictions and those of Zanon et al. (2018) (Supplementary Information: S6). Zanon et al. (2018) visually compare their interpolated modern tree cover map and the observed tree cover from Hansen et al. (2013), but they do not report a correlation or R^2 value. However, the correlation values for Serge et al. (2023) broadly align with those reported comparing REVEALS tree cover estimates, with observed tree cover derived from Hansen et al. (2013) ($R^2 = 0.15$; correlation ~ 0.4).

https://doi.org/10.5194/egusphere-2024-1523
Preprint. Discussion started: 27 May 2024

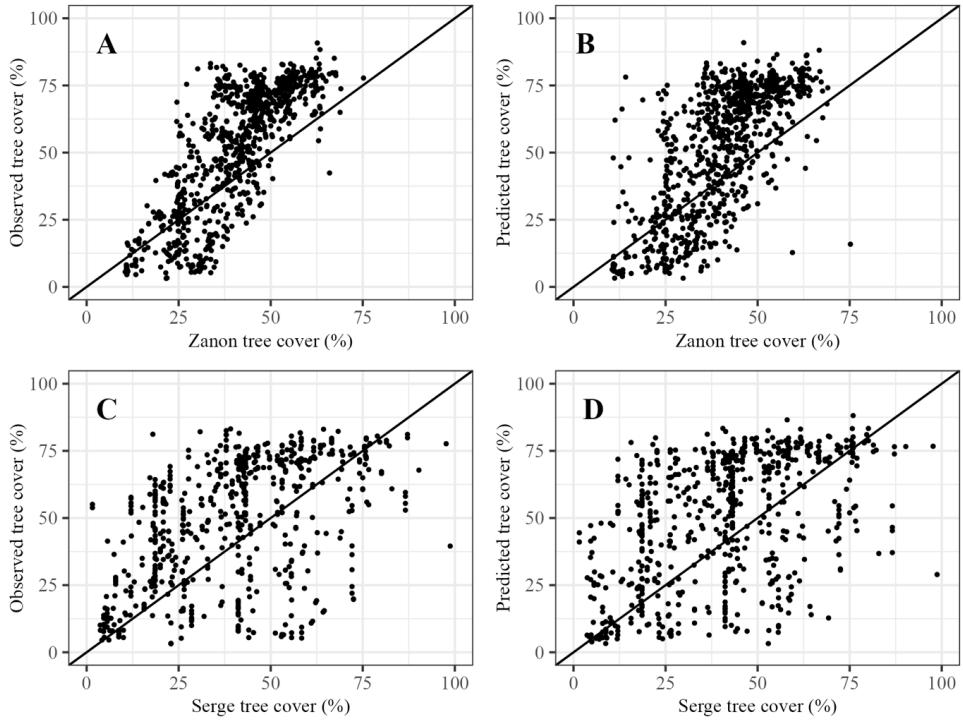

Figure 4: Modern tree cover from Zanon et al (2018) compared to (A) observed tree cover and (B) our predicted tree cover. Modern tree cover from Serge et al. (2023) compared to (C) observed tree cover values and (D) our predicted tree cover.

3.2 Holocene changes in tree cover

We applied the tree cover model to reconstruct Holocene changes in tree cover at individual sites (see section *Data and code availability* for binned reconstructions at site level). The median tree cover value, considering Europe as a whole, increased rapidly between 12,000 to ca. 8,500 cal. BP, and then more slowly to a peak at ca. 6,500 cal. BP. Median tree cover declined overall between 6,500 cal. BP and 4,000 cal. BP, albeit with some variability. Median tree cover declined steadily to present-day levels after ca. 4,000 cal. BP (Fig. 5A). This same pattern is shown when considering changes in mean tree cover (Supplementary Information: S7) and different LOESS smoothing (R package *locfit* Loader, 2020) of the median tree cover value (Fig. 5B). The rapid warming at the end of the Younger Dryas (Alley, 2000; Cheng et al., 2020), and the changes associated with the 8,200 cal. BP event (Alley et al., 1997; Alley and Ágústsdóttir, 2005) and the 4,200 cal. BP event (e.g. Weiss et al., 1993; Bini et al., 2019) are not apparent at this pan-European scale.

https://doi.org/10.5194/egusphere-2024-1523
Preprint. Discussion started: 27 May 2024

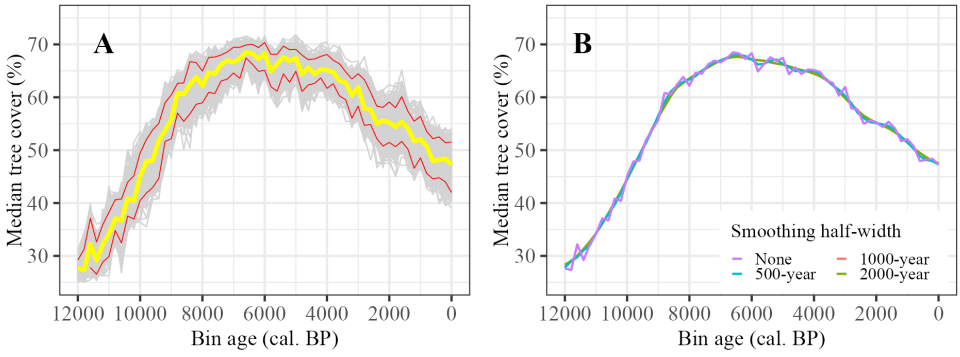

Figure 5: A - Median reconstructed tree cover for Europe from 12,000 to 0 cal. BP, with 95% confidence intervals for 1000 bootstrap resampling of records; B - Median reconstructed tree cover for Europe from 12,000 to 0 cal. BP, with differing LOESS regression smoothing half-widths.

These pan-European trends mask considerable regional variability in tree cover at any given time and in trends through time (see Supplementary Information: S8, for gridded maps of reconstructed tree cover). To examine these trends, we consider four biogeographical regions for which there is sufficient data: the Atlantic, Boreal, Continental and Mediterranean regions (Figure 2D; Supplementary Information: S9).

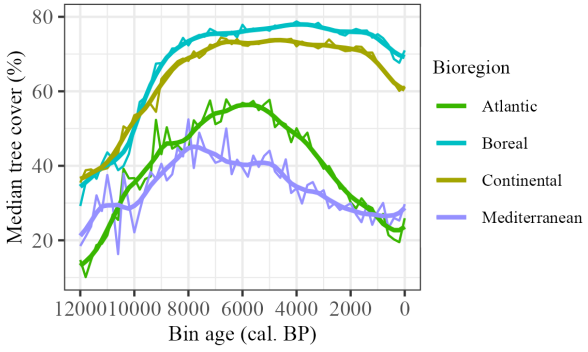

Figure 6: Median tree cover values, for selected biogeographical regions. Smoothed lines reflect LOESS fitted regression with 1000-year halfwidth.

The increase in tree cover at the beginning of the Holocene is shown in all four regions, but the trajectories are different (Fig. 6). There is an immediate rapid increase in the Atlantic region, but the increase is initially slow in the Boreal and Continental regions and only becomes more rapid after ca. 11,000 cal. BP in the Continental region and after ca. 10,300 cal. BP in the Boreal region. The initial increase in the Mediterranean region is interrupted by a decline between 11,000 and 10,000 cal. BP and only begins to increase again after ca. 9,800 cal. BP. The maximum in tree cover in the Mediterranean region is reached at ca. 8,000 cal. BP. After this there is a decline towards present-day levels, although this is interrupted by intervals of relative stability e.g. between ca. 6,000 and 5,000 cal. BP, again between 4,000 and 3,000 cal. BP and in the most recent millennium. There is also a well-defined

https://doi.org/10.5194/egusphere-2024-1523
Preprint. Discussion started: 27 May 2024

maximum in tree cover in the Atlantic region, but this occurs at ca. 6,000 cal. BP. The subsequent decline is gradual until the last ca. 500 years. The maximum in tree cover is broader in the Continental and Boreal regions, with high levels of tree cover characteristic of the entire interval between ca. 8,000 and 1,000 cal. BP although the absolute maximum occurs at ca. 6,400 cal. BP in the Continental region and not until ca. 4,000 cal. BP in the Boreal region. Both regions are characterised by a rapid decline in the last millennium.

This broad pattern of increase, mid-Holocene maximum and then decline to present is consistent with previous reconstructions (Fig. 7). Initial levels of tree cover are similar in the three reconstructions (ca. 27.5-30%), but the increase in tree cover is more rapid in the Zanon et al. (2018) and Serge et al. (2023) reconstructions. Our reconstructed maximum cover in somewhat lower (ca. 5-10%) than shown by the other reconstructions, but the mid-Holocene timing is broadly consistent across all of the reconstructions (although Zanon et al. (2018) show a double peak in tree cover, with an earlier peak at ca. 9,000 cal. BP) within the limitations of the age models and binning intervals used (see Supplementary Information: S10 and S11). These broad trends are maintained when calculating tree cover from Zanon et al. (2018) and Serge et al. (2023) data such that only a single value per grid cell is permitted in the calculation of the median (Supplementary Information: S12). The biggest difference between our reconstructed tree cover and previous studies is that the decrease post-ca. 2000 cal. BP is less abrupt. Both Zanon et al (2018) and Serge et al (2023) show a steep decline to levels (ca. 35%) similar to those at the beginning of the Holocene whereas we show a decline to only ca. 47.5%. Based on pollen record locations and a 5km^2 buffer, observed modern median tree cover is 46%, which suggests our estimated decline is more realistic.

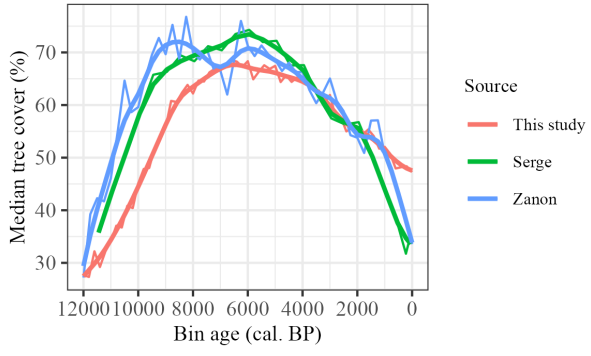

Figure 7: Reconstructed median tree cover compared to equivalent extracted tree cover medians for Serge et al. (2023) and Zanon et al (2018). Smoothed lines reflect LOESS fitted regression with 1000-year halfwidth.

The three reconstructions also show some similarities at a sub-regional scale (Fig. 8), although comparison is more difficult because of differences in methodologies and coverage. As is the case for the pan-European comparison, Zanon et al. (2018) and Serge et al. (2023) generally show higher tree cover than our reconstruction. The peak tree cover in the Atlantic region occurs earlier in these

https://doi.org/10.5194/egusphere-2024-1523
Preprint. Discussion started: 27 May 2024

reconstructions, and Zanon et al. (2018) also show an earlier peak in the Continental region. The later Holocene decline in tree cover is similar across all three reconstructions in the Atlantic region, but the previous reconstructions show a steeper decline in the Boreal and Continental regions. The biggest differences between the three reconstructions is in the Mediterranean region, where Serge et al. (2023) show a pronounced peak reaching 60% cover at ca. 5,500 cal. BP, whereas the other two reconstructions show comparatively muted changes in tree cover at around 40% throughout the mid- to late Holocene. This probably reflects differences in data coverage between Serge et al. (2023) and the other two reconstructions.

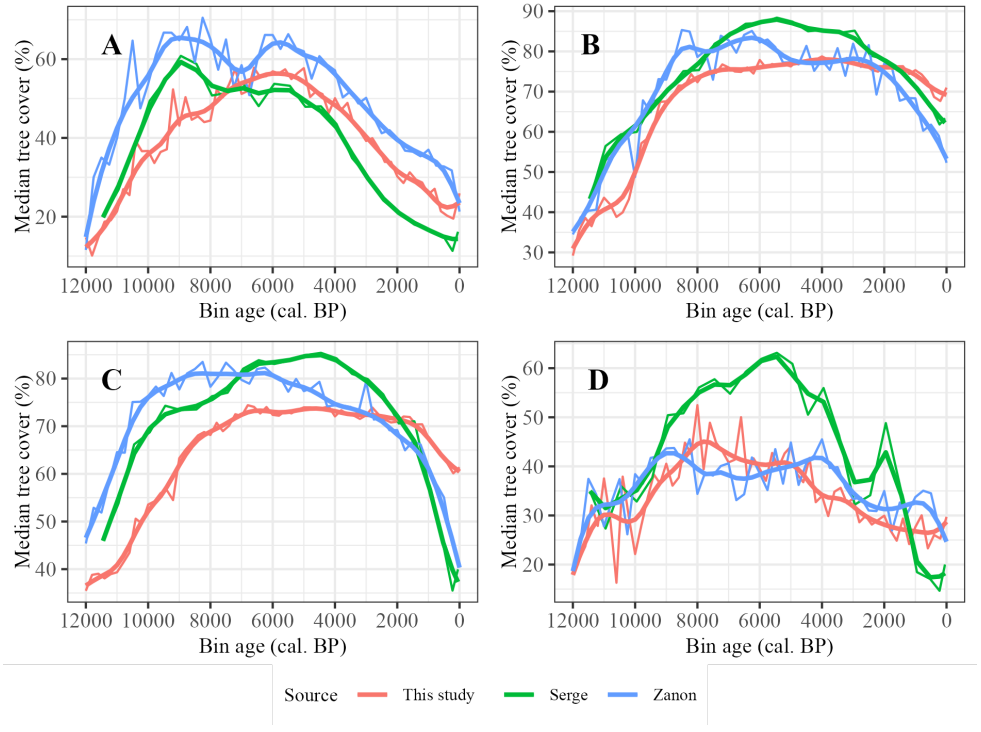

Figure 8: Reconstructed median tree cover compared to equivalent extracted tree cover medians for Serge et al. (2023) and Zanon et al. (2018), for selected modern biogeographical regions. Smoothed lines reflect LOESS fitted regression with 1000-year halfwidth. A – Atlantic; B- Boreal; C- Continental; D – Mediterranean.

Although the overall European median tree cover partially reflects the quantity of data for each region, recalculating the European level median tree cover based on just the four biogeographical regions of focus has very little material effect on the overall pattern of median tree cover for each reconstruction (Supplementary Information: S13).

https://doi.org/10.5194/egusphere-2024-1523
Preprint. Discussion started: 27 May 2024

4. Discussion

Our reconstructions show that tree cover peaked in the mid-Holocene period, with median tree cover ca. 40% greater than at the beginning of the Holocene. This general pattern is shown by the REVEALS and MAT reconstructions, and is also visible in plant functional type (Davis et al., 2015) and pseudo-biomization reconstructions of vegetation cover (Fyfe et al., 2015). There are differences in the timing and extent of changes between regions, although the general pattern of increase, mid-Holocene peak and subsequent decline is shown everywhere. There are some differences between our reconstructions and those from other studies. Firstly, the maximum tree cover from our reconstructions is around 5-10% less than the maximum calculated from the other reconstructions. This could reflect the conservative nature of our modern-day tree cover model, which underestimates tree cover at the high end despite the application of quantitative mapping adjustment to model predictions. However, Zanon et al. (2018) also underestimate tree cover at high levels of tree cover. Alternatively, the difference may reflect the exclusion of higher elevation records from fossil dataset in order to minimise the impact of upslope pollen transport, which was not done in the other two reconstructions and would tend to reduce overall median tree cover. Secondly, the timings of peak tree cover vary between the reconstructions, with the MAT-based estimate peaking earlier and the REVEALS estimate later than shown in our reconstruction. These differences likely reflect differences in coverage through time and differences in the binning procedure. The major difference at the pan-European scale is the reduction in tree cover from ca. 2000 cal. BP to present, which is less marked in our reconstructions and more consistent with observed tree cover. Observed tree cover values exclude areas occupied by non-natural vegetation, such as built areas or areas dominated by crops. We account for this in defining modern source areas in our model, since the pollen only provides evidence of the natural vegetation. Failure to account for anthropogenic land-use, which has increased substantially over the past 1000 years (Klein Goldewijk et al., 2017) would result in a steeper decline in tree cover, as seen in the other two reconstructions.

We took an inclusive approach in defining the modern training data and for the fossil records to maximise spatial coverage. The inclusion of bogs, for example, reduced the goodness-of-fit of the model slightly but resulted in much better spatial coverage. Conversely, the exclusion of high-elevation sites did not have a major impact on spatial coverage but was necessary to improve model fit because of the tendency for upslope transport of pollen in mountainous areas. Nevertheless, there are still areas of Europe which lack data, or where there is a mismatch in coverage between the modern and fossil records. Improved sampling of such areas would enhance our confidence in the reconstructions of Holocene tree cover.

Our reconstructions are consistent with understanding of Holocene climate patterns. The rapid increase in tree cover at the beginning of the Holocene shown in the pan-European reconstruction and in most

https://doi.org/10.5194/egusphere-2024-1523
Preprint. Discussion started: 27 May 2024

of the sub-regional reconstructions reflects the marked warming after the Younger Dryas. This warming is less pronounced and more gradual in the Mediterranean region, consistent with the fact that the Younger Dryas cool interval is not strongly registered over much of this region (Bottema, 1995; Cruz-Silva et al., 2023). Subsequent pan-European changes in tree cover broadly reflect changes in growing season temperature, which itself is a reflection of orbitally-forced changes in summer insolation. However, modelling studies have shown that the timing of maximum warmth during the Holocene in Europe was delayed compared to the maximum of insolation forcing as a consequence of feedbacks associated with the presence of the Laurentide and Scandinavian ice sheets (Renssen et al., 2009; Blaschek and Renssen, 2013; Zhang et al., 2016, 2018). However, they consistently show that the warming was delayed in the region bordering the Atlantic (and northwest Europe more generally) by ca. 2,000 years compared to more continental regions, consistent with our reconstructions. The more muted changes in tree cover in the Mediterranean region compared to other regions of Europe is consistent with previous reconstructions and is partly explained by the fact that these changes are largely driven by changes in precipitation and precipitation seasonality (Cruz-Silva et al., 2023). The late Holocene decline in tree cover is consistent with the orbitally-driven cooling. However, the more rapid decline in tree cover during the last millennium shown in the Boreal and Continental regions, and shown more dramatically in the Zanon et al. (2018) and Serge et al. (2023) reconstructions, is more difficult to explain - transient model simulations of the response to changes in orbital and greenhouse gas forcing (e.g. Liu et al., 2009; Zhang et al., 2016; Braconnot et al., 2019; Dallmeyer et al., 2020) generally indicate muted changes in either summer or winter temperatures during the most recent millennia. Human influence on the landscape may help explain these later reductions in tree cover. Although human influence on the landscape has been identified in some regions of Europe from 6,000 cal. BP onwards (e.g. Roberts et al., 2018; Zapolska et al., 2023), rapid population growth occurred only during the past 2000 years (Klein Goldewijk et al., 2010, 2017). The recent decline in tree cover may therefore reflect increasing human influence on the landscape in some regions (see e.g. Marquer et al., 2017; Roberts et al., 2019). However, more formal modelling of these relationships is required to assign the impact of each on tree cover in recent millennia more confidently.

Our simple modelling approach yields a reasonably robust picture of changes in tree cover through the Holocene, largely consistent with known changes in climate. It is less data-demanding that the REVEALS approach. Serge et al. (2023) have pointed out that lack of reliable information on species RPP values is likely to lead to less accurate reconstructions. Even in Europe, there is limited RPP data and, as the comparison of reconstructions based on 31 and 46 species shows, some of that data may not be reliable. RPP data is more limited in many other regions of the world (Harrison et al., 2020). Given this, our simple modelling approach provides an alternative method that could be applied to reconstruct tree cover globally. It is difficult to compare our reconstructions with the MAT-based approach of Zanon et al. (2018) since they do not provide individual site estimates and it is therefore not possible to

https://doi.org/10.5194/egusphere-2024-1523
Preprint. Discussion started: 27 May 2024

determine the degree to which the patterns are influenced by the spatial and temporal interpolations they applied. Nevertheless, our simple approach overcomes the methodological issues associated with MAT, such how to measure the degree of analogy between assemblages, how to deal with non-analogues, and the sensitivity of the reconstructions to the number of analogues used. Thus, given the existence of global modern pollen training data sets and good remote-sensing based modern estimates of tree cover, our approach could be applied to other regions of the world to generate robust reconstructions of tree cover.

5. Conclusions

We have made use of modern pollen data and maps of tree cover percentage to build a simple model of tree cover. We then applied this model to fossil pollen records to reconstruct tree cover at a site level during the Holocene across Europe. At a pan-European level, tree cover increased from the early Holocene to the mid-Holocene, and then subsequently declined to the present day. There are regional variations in the speed of the initial increase, the timing of maximum tree cover, and the form of the subsequent decline. Our simple approach produces similar reconstructions of the trends in tree cover during the Holocene reconstructed using more complex methods, and thus provides a less data-demanding approach that could be used in other regions of the world.

6. Code and data availability

The SMPDSv2 modern pollen database is available from the University of Reading Research Data Archive (https://researchdata.reading.ac.uk/389/) and/or via https://github.com/special-uor/smpds?tab=readme-ov-file

Metadata updates to SMPDSv2, including basin size updates are available at https://doi.org/10.5281/zenodo.11220915

The SPECIAL.EPD fossil pollen database is available from the University of Reading Research Data Archive (https://researchdata.reading.ac.uk/1295/)

The code used in generating tree cover, binned site-based reconstructions of tree cover, the code as cross-analysis of the data, and species categorisation tables are available at https://doi.org/10.5281/zenodo.11220915

7. Supplemental link

The supplement related to this article is available online.

https://doi.org/10.5194/egusphere-2024-1523
Preprint. Discussion started: 27 May 2024

8. Author contribution

LS, SPH and MVL conceived this study. LS carried out the analysis. LS and SPH wrote the first draft of the manuscript and all authors contributed to the final version.

9. Competing interests

The authors declare that they have no conflict of interest.

10. Acknowledgments

We thank colleagues in the Leverhulme Centre for Wildfires, Environment and Society (https://centreforwildfires.org/) and from the SPECIAL group at the University of Reading (https://research.reading.ac.uk/palaeoclimate/) for discussions during the development of this work.

11. Financial support

LS acknowledges support from the Leverhulme Centre for Wildfires, Environment and Society. SPH acknowledges support from the ERC-funded project GC 2.0 (Global Change 2.0: Unlocking the past for a clearer future; grant number 694481).

https://doi.org/10.5194/egusphere-2024-1523
Preprint. Discussion started: 27 May 2024

12. References

Abis, B. and Brovkin, V.: Environmental conditions for alternative tree-cover states in high latitudes, Biogeosciences, 14, 511–527, https://doi.org/10.5194/bg-14-511-2017, 2017.

Akaike, H.: A New Look at the Statistical Model Identification, IEEE Trans. Automat. Contr., 19, 716–723, https://doi.org/10.1109/TAC.1974.1100705, 1974.

Alkama, R. and Cescatti, A.: Biophysical climate impacts of recent changes in global forest cover, Science, 351, 600–604, https://doi.org/10.1126/science.aac8083, 2016.

Alley, R. B.: The Younger Dryas cold interval as viewed from central Greenland, Quat. Sci. Rev., 19, 213–226, https://doi.org/10.1016/S0277-3791(99)00062-1, 2000.

Alley, R. B. and Ágústsdóttir, A. M.: The 8k event: Cause and consequences of a major Holocene abrupt climate change, Quat. Sci. Rev., 24, 1123–1149, https://doi.org/10.1016/j.quascirev.2004.12.004, 2005.

Alley, R. B., Mayewski, P. A., Sowers, T., Stuiver, M., Taylor, K. C., and Clark, P. U.: Holocene climatic instability: A prominent, widespread event 8200 yr ago, Geology, 25, 483–486, https://doi.org/10.1130/0091-7613(1997)025<0483:HCIAPW>2.3.CO;2, 1997.

Baston, D.: exactextractr: Fast Extraction from Raster Datasets using Polygons, https://isciences.gitlab.io/exactextractr/, 2023.

Bini, M., Zanchetta, G., Perşoiu, A., Cartier, R., Català, A., Cacho, I., Dean, J. R., Di Rita, F., Drysdale, R. N., Finnè, M., Isola, I., Jalali, B., Lirer, F., Magri, D., Masi, A., Marks, L., Mercuri, A. M., Peyron, O., Sadori, L., Sicre, M.-A., Welc, F., Zielhofer, C., and Brisset, E.: The 4.2 ka BP Event in the Mediterranean region: an overview, Clim. Past, 15, 555–577, https://doi.org/10.5194/cp-15-555-2019, 2019.

Blaschek, M. and Renssen, H.: The Holocene thermal maximum in the Nordic Seas: the impact of Greenland Ice Sheet melt and other forcings in a coupled atmosphere–sea-ice–ocean model, Clim. Past, 9, 1629–1643, https://doi.org/10.5194/cp-9-1629-2013, 2013.

Bonan, G. B.: Forests and Climate Change: Forcings, Feedbacks, and the Climate Benefits of Forests, Science, 320, 1444–1449, https://doi.org/10.1126/science.1155121, 2008.

Bottema, S.: The Younger Dryas in the Eastern Mediterranean, Quat. Sci. Rev., 14, 883–891, https://doi.org/10.1016/0277-3791(95)00069-0, 1995.

Braconnot, P., Zhu, D., Marti, O., and Servonnat, J.: Strengths and challenges for transient Mid- to Late Holocene simulations with dynamical vegetation, Clim. Past, 15, 997–1024, https://doi.org/10.5194/cp-15-997-2019, 2019.

Bradshaw, R. H. W. and Webb, T.: Relationships between Contemporary Pollen and Vegetation Data from Wisconsin and Michigan, USA, Ecology, 66, 721–737, https://doi.org/10.2307/1940533, 1985.

Buchhorn, M., Smets, B., Bertels, L., de Roo, B., Lesiv, M., Tsendbazar, N.-E., Li, L., and Tarko, A.: Copernicus Global Land Service: Land Cover 100m: collection 3: epoch 2015: Globe, https://doi.org/https://doi.org/10.5281/zenodo.3939038, 2020a.

https://doi.org/10.5194/egusphere-2024-1523
Preprint. Discussion started: 27 May 2024

Buchhorn, M., Smets, B., Bertels, L., Roo, B. De, Lesiv, M., Tsendbazar, N.-E., Herold, M., and Fritz, S.: Copernicus Global Land Service: Land Cover 100m: collection 3: epoch 2016: Globe, https://doi.org/10.5281/zenodo.3518026, September 2020b.

Buchhorn, M., Smets, B., Bertels, L., Roo, B. De, Lesiv, M., Tsendbazar, N.-E., Herold, M., and Fritz, S.: Copernicus Global Land Service: Land Cover 100m: collection 3: epoch 2017: Globe, https://doi.org/10.5281/zenodo.3518036, September 2020c.

Buchhorn, M., Smets, B., Bertels, L., Roo, B. De, Lesiv, M., Tsendbazar, N.-E., Herold, M., and Fritz, S.: Copernicus Global Land Service: Land Cover 100m: collection 3: epoch 2018: Globe, https://doi.org/10.5281/zenodo.3518038, September 2020d.

Buchhorn, M., Smets, B., Bertels, L., Roo, B. De, Lesiv, M., Tsendbazar, N.-E., Herold, M., and Fritz, S.: Copernicus Global Land Service: Land Cover 100m: collection 3: epoch 2019: Globe, https://doi.org/10.5281/zenodo.3939050, September 2020e.

Bunting, M. J. and Farrell, M.: Do Local Habitat Conditions Affect Estimates of Relative Pollen Productivity and Source Area in Heathlands?, Front. Ecol. Evol., 10, https://doi.org/10.3389/fevo.2022.787345, 2022.

Bunting, M. J., Twiddle, C. L., and Middleton, R.: Using models of pollen dispersal and deposition in hilly landscapes: Some possible approaches, Palaeogeogr. Palaeocl., 259, 77–91, https://doi.org/10.1016/j.palaeo.2007.03.051, 2008.

Cheng, H., Zhang, H., Spötl, C., Baker, J., Sinha, A., Li, H., Bartolomé, M., Moreno, A., Kathayat, G., Zhao, J., Dong, X., Li, Y., Ning, Y., Jia, X., Zong, B., Ait Brahim, Y., Pérez-Mejías, C., Cai, Y., Novello, V. F., Cruz, F. W., Severinghaus, J. P., An, Z., and Edwards, R. L.: Timing and structure of the Younger Dryas event and its underlying climate dynamics, Proc. Natl. Acad. Sci. U.S.A, 117, 23408–23417, https://doi.org/10.1073/pnas.2007869117, 2020.

Cox, D. R. and Snell, E. J.: Analysis of Binary Data, 2nd Edition., Chapman & Hall, 1989.

Cribari-Neto, F. and Zeileis, A.: Beta Regression in *R*, J. Stat. Softw., 34, https://doi.org/10.18637/jss.v034.i02, 2010.

Cruz-Silva, E., Harrison, S. P., Prentice, I. C., Marinova, E., Bartlein, P. J., Renssen, H., and Zhang, Y.: Pollen-based reconstructions of Holocene climate trends in the eastern Mediterranean region, Clim. Past, 19, 2093–2108, https://doi.org/10.5194/cp-19-2093-2023, 2023.

Dallmeyer, A., Claussen, M., Lorenz, S. J., and Shanahan, T.: The end of the African humid period as seen by a transient comprehensive Earth system model simulation of the last 8000 years, Clim. Past, 16, 117–140, https://doi.org/10.5194/cp-16-117-2020, 2020.

Davis, B. A. S., Collins, P. M., and Kaplan, J. O.: The age and post-glacial development of the modern European vegetation: a plant functional approach based on pollen data, Veg. Hist. Archaeobot., 24, 303–317, https://doi.org/10.1007/s00334-014-0476-9, 2015.

European Environment Agency: Biogeographical regions, https://sdi.eea.europa.eu/catalogue/srv/api/records/11db8d14-f167-4cd5-9205-95638dfd9618, 2016.

https://doi.org/10.5194/egusphere-2024-1523
Preprint. Discussion started: 27 May 2024

Fall, P. L.: Spatial patterns of atmospheric pollen dispersal in the Colorado Rocky Mountains, USA, Rev. Palaeobot. Palynol., 74, 293–313, https://doi.org/10.1016/0034-6667(92)90013-7, 1992.

FAO: Global Forest Resources Assessment 2020, FAO, https://doi.org/10.4060/ca9825en, 2020.

Fyfe, R. M., Woodbridge, J., and Roberts, N.: From forest to farmland: pollen-inferred land cover change across Europe using the pseudobiomization approach, Glob. Chang. Biol., 21, 1197–1212, https://doi.org/10.1111/gcb.12776, 2015.

Gaillard, M.-J., Sugita, S., Mazier, F., Trondman, A.-K., Broström, A., Hickler, T., Kaplan, J. O., Kjellström, E., Kokfelt, U., Kuneš, P., Lemmen, C., Miller, P., Olofsson, J., Poska, A., Rundgren, M., Smith, B., Strandberg, G., Fyfe, R., Nielsen, A. B., Alenius, T., Balakauskas, L., Barnekow, L., Birks, H. J. B., Bjune, A., Björkman, L., Giesecke, T., Hjelle, K., Kalnina, L., Kangur, M., van der Knaap, W. O., Koff, T., Lagerås, P., Latałowa, M., Leydet, M., Lechterbeck, J., Lindbladh, M., Odgaard, B., Peglar, S., Segerström, U., von Stedingk, H., and Seppä, H.: Holocene land-cover reconstructions for studies on land cover-climate feedbacks, Clim. Past, 6, 483–499, https://doi.org/10.5194/cp-6-483-2010, 2010.

Githumbi, E., Fyfe, R., Gaillard, M.-J., Trondman, A.-K., Mazier, F., Nielsen, A.-B., Poska, A., Sugita, S., Woodbridge, J., Azuara, J., Feurdean, A., Grindean, R., Lebreton, V., Marquer, L., Nebout-Combourieu, N., Stančikaitė, M., Tanţău, I., Tonkov, S., and Shumilovskikh, L.: European pollen-based REVEALS land-cover reconstructions for the Holocene: methodology, mapping and potentials, Earth Syst. Sci. Data, 14, 1581–1619, https://doi.org/10.5194/essd-14-1581-2022, 2022.

Gudmundsson, L., Bremnes, J. B., Haugen, J. E., and Engen-Skaugen, T.: Technical Note: Downscaling RCM precipitation to the station scale using statistical transformations - a comparison of methods, Hydrol. Earth Syst. Sci., 16, 3383–3390, https://doi.org/10.5194/hess-16-3383-2012, 2012.

Guiot, J.: Methodology of the last climatic cycle reconstruction in France from pollen data, Palaeogeogr. Palaeocl., 80, 49–69, https://doi.org/10.1016/0031-0182(90)90033-4, 1990.

Hansen, M. C., Potapov, P. V., Moore, R., Hancher, M., Turubanova, S. A., Tyukavina, A., Thau, D., Stehman, S. V., Goetz, S. J., Loveland, T. R., Kommareddy, A., Egorov, A., Chini, L., Justice, C. O., and Townshend, J. R. G.: High-Resolution Global Maps of 21st-Century Forest Cover Change, Science, 342, 850–853, https://doi.org/10.1126/science.1244693, 2013.

Harrison, S.P., Egbudom, M.A., Liu, M., Cruz-Silva, E. and Sweeney, L.F.: The SPECIAL EPD Database: an expanded resource to document changes in vegetation and climate from pollen records from Europe, the Middle East and western Eurasia. University of Reading. Dataset. https://doi.org/10.17864/1947.001295, 2024

Heaton, T. J., Köhler, P., Butzin, M., Bard, E., Reimer, R. W., Austin, W. E. N., Bronk Ramsey, C., Grootes, P. M., Hughen, K. A., Kromer, B., Reimer, P. J., Adkins, J., Burke, A., Cook, M. S., Olsen, J., and Skinner, L. C.: Marine20—The Marine Radiocarbon Age Calibration Curve (0–55,000 cal BP), Radiocarbon, 62, 779–820, https://doi.org/10.1017/RDC.2020.68, 2020.

https://doi.org/10.5194/egusphere-2024-1523
Preprint. Discussion started: 27 May 2024

Hill, J. L. and Curran, P. J.: Area, shape and isolation of tropical forest fragments: effects on tree species diversity and implications for conservation, J. Biogeogr., 30, 1391–1403, https://doi.org/10.1046/j.1365-2699.2003.00930.x, 2003.

Hill, M. O.: Diversity and Evenness: A Unifying Notation and Its Consequences, Ecology, 54, 427–432, https://doi.org/10.2307/1934352, 1973.

Jackson, S. T. and Williams, J. W.: Modern Analogs in Quaternary Paleoecology: Here Today, Gone Yesterday, Gone Tomorrow?, Annu. Rev. Earth Pl. Sc., 32, 495–537, https://doi.org/10.1146/annurev.earth.32.101802.120435, 2004.

Jactel, H., Bauhus, J., Boberg, J., Bonal, D., Castagneyrol, B., Gardiner, B., Gonzalez-Olabarria, J. R., Koricheva, J., Meurisse, N., and Brockerhoff, E. G.: Tree Diversity Drives Forest Stand Resistance to Natural Disturbances, Curr. For. Rep., 3, 223–243, https://doi.org/10.1007/s40725-017-0064-1, 2017.

Klein Goldewijk, K., Beusen, A., and Janssen, P.: Long-term dynamic modeling of global population and built-up area in a spatially explicit way: HYDE 3.1, Holocene, 20, 565–573, https://doi.org/10.1177/0959683609356587, 2010.

Klein Goldewijk, K., Beusen, A., Doelman, J., and Stehfest, E.: Anthropogenic land use estimates for the Holocene – HYDE 3.2, Earth Syst. Sci. Data, 9, 927–953, https://doi.org/10.5194/essd-9-927-2017, 2017.

Leite-Filho, A. T., Costa, M. H., and Fu, R.: The southern Amazon rainy season: The role of deforestation and its interactions with large-scale mechanisms, Int. J. Climatol, 40, 2328–2341, https://doi.org/10.1002/joc.6335, 2020.

Liu, Z., Otto-Bliesner, B. L., He, F., Brady, E. C., Tomas, R., Clark, P. U., Carlson, A. E., Lynch-Stieglitz, J., Curry, W., Brook, E., Erickson, D., Jacob, R., Kutzbach, J., and Cheng, J.: Transient Simulation of Last Deglaciation with a New Mechanism for Bølling-Allerød Warming, Science, 325, 310–314, https://doi.org/10.1126/science.1171041, 2009.

Loader, C.: Locfit: Local regression, likelihood and density estimation, http://cran.r-project.org/package=locfit%5Cnpapers2://publication/uuid/E5C68958-7122-4093-A8E2-3108F9DF726A, 2020.

Markgraf, V.: Pollen Dispersal in a Mountain Area, Grana, 19, 127–146, https://doi.org/10.1080/00173138009424995, 1980.

Marquer, L., Gaillard, M.-J., Sugita, S., Trondman, A.-K., Mazier, F., Nielsen, A. B., Fyfe, R. M., Odgaard, B. V., Alenius, T., Birks, H. J. B., Bjune, A. E., Christiansen, J., Dodson, J., Edwards, K. J., Giesecke, T., Herzschuh, U., Kangur, M., Lorenz, S., Poska, A., Schult, M., and Seppä, H.: Holocene changes in vegetation composition in northern Europe: why quantitative pollen-based vegetation reconstructions matter, Quat. Sci. Rev., 90, 199–216, https://doi.org/10.1016/j.quascirev.2014.02.013, 2014.

Marquer, L., Gaillard, M.-J., Sugita, S., Poska, A., Trondman, A.-K., Mazier, F., Nielsen, A. B., Fyfe, R. M., Jönsson, A. M., Smith, B., Kaplan, J. O., Alenius, T., Birks, H. J. B., Bjune, A. E., Christiansen,

https://doi.org/10.5194/egusphere-2024-1523
Preprint. Discussion started: 27 May 2024

J., Dodson, J., Edwards, K. J., Giesecke, T., Herzschuh, U., Kangur, M., Koff, T., Latałowa, M., Lechterbeck, J., Olofsson, J., and Seppä, H.: Quantifying the effects of land use and climate on Holocene vegetation in Europe, Quat. Sci. Rev., 171, 20–37, https://doi.org/10.1016/j.quascirev.2017.07.001, 2017.

Moreira, F., Rego, F. C., and Ferreira, P. G.: Temporal (1958–1995) pattern of change in a cultural landscape of northwestern Portugal: implications for fire occurrence, Landsc. Ecol., 16, 557–567, https://doi.org/10.1023/A:1013130528470, 2001.

Moyes, A. B., Germino, M. J., and Kueppers, L. M.: Moisture rivals temperature in limiting photosynthesis by trees establishing beyond their cold-edge range limit under ambient and warmed conditions, New Phytol., 207, 1005–1014, https://doi.org/10.1111/nph.13422, 2015.

Nielsen, A. B., Giesecke, T., Theuerkauf, M., Feeser, I., Behre, K.-E., Beug, H.-J., Chen, S.-H., Christiansen, J., Dörfler, W., Endtmann, E., Jahns, S., de Klerk, P., Kühl, N., Latałowa, M., Odgaard, B. V., Rasmussen, P., Stockholm, J. R., Voigt, R., Wiethold, J., and Wolters, S.: Quantitative reconstructions of changes in regional openness in north-central Europe reveal new insights into old questions, Quat. Sci. Rev., 47, 131–149, https://doi.org/10.1016/j.quascirev.2012.05.011, 2012.

Ortu, E., de Beaulieu, J. L., Caramiello, R., and Siniscalco, C.: Late Glacial and Holocene vegetation dynamics at various altitudes in the Ellero Valley, Maritime Alps, northwestern Italy, Ecoscience, 15, 200–212, https://doi.org/10.2980/15-2-2926, 2008.

Ortu, E., David, F., and Peyron, O.: Pollen-inferred palaeoclimate reconstruction in the Alps during the Lateglacial and the early Holocene: how to estimate the effect of elevation and local parameters, J. Quat. Sci., 25, 651–661, https://doi.org/10.1002/jqs.1335, 2010.

Overpeck, J. T., Webb, T., and Prentice, I. C.: Quantitative Interpretation of Fossil Pollen Spectra: Dissimilarity Coefficients and the Method of Modern Analogs, Quat. Res., 23, 87–108, https://doi.org/10.1016/0033-5894(85)90074-2, 1985.

Prentice, C.: Records of vegetation in time and space: the principles of pollen analysis, in: Vegetation history, Springer Netherlands, Dordrecht, 17–42, https://doi.org/10.1007/978-94-009-3081-0_2, 1988.

Prentice, I. C.: Pollen Representation, Source Area, and Basin Size: Toward a Unified Theory of Pollen Analysis, Quat. Res., 23, 76–86, https://doi.org/10.1016/0033-5894(85)90073-0, 1985.

Prentice, I. C. and Webb, T.: Pollen percentages, tree abundances and the Fagerlind effect, J. Quat. Sci., 1, 35–43, https://doi.org/10.1002/jqs.3390010105, 1986.

R Core Team: R: A Language and Environment for Statistical Computing, R Foundation for Statistical Computing, Vienna, Austria, 2022.

Reimer, P. J., Austin, W. E. N., Bard, E., Bayliss, A., Blackwell, P. G., Bronk Ramsey, C., Butzin, M., Cheng, H., Edwards, R. L., Friedrich, M., Grootes, P. M., Guilderson, T. P., Hajdas, I., Heaton, T. J., Hogg, A. G., Hughen, K. A., Kromer, B., Manning, S. W., Muscheler, R., Palmer, J. G., Pearson, C., van der Plicht, J., Reimer, R. W., Richards, D. A., Scott, E. M., Southon, J. R., Turney, C. S. M., Wacker, L., Adolphi, F., Büntgen, U., Capano, M., Fahrni, S. M., Fogtmann-Schulz, A., Friedrich, R., Köhler,

https://doi.org/10.5194/egusphere-2024-1523
Preprint. Discussion started: 27 May 2024

P., Kudsk, S., Miyake, F., Olsen, J., Reinig, F., Sakamoto, M., Sookdeo, A., and Talamo, S.: The IntCal20 Northern Hemisphere Radiocarbon Age Calibration Curve (0–55 cal kBP), Radiocarbon, 62, 1–33, https://doi.org/10.1017/rdc.2020.41, 2020.

Renssen, H., Seppä, H., Heiri, O., Roche, D. M., Goosse, H., and Fichefet, T.: The spatial and temporal complexity of the Holocene thermal maximum, Nat. Geosci., 2, 411–414, https://doi.org/10.1038/ngeo513, 2009.

Roberts, C. N., Woodbridge, J., Palmisano, A., Bevan, A., Fyfe, R., and Shennan, S.: Mediterranean landscape change during the Holocene: Synthesis, comparison and regional trends in population, land cover and climate, Holocene, 29, 923–937, https://doi.org/10.1177/0959683619826697, 2019.

Roberts, N., Fyfe, R. M., Woodbridge, J., Gaillard, M.-J., Davis, B. A. S., Kaplan, J. O., Marquer, L., Mazier, F., Nielsen, A. B., Sugita, S., Trondman, A.-K., and Leydet, M.: Europe's lost forests: a pollen-based synthesis for the last 11,000 years, Sci. Rep., 8, 716, https://doi.org/10.1038/s41598-017-18646-7, 2018.

Serge, M., Mazier, F., Fyfe, R., Gaillard, M.-J., Klein, T., Lagnoux, A., Galop, D., Githumbi, E., Mindrescu, M., Nielsen, A., Trondman, A.-K., Poska, A., Sugita, S., Woodbridge, J., Abel-Schaad, D., Åkesson, C., Alenius, T., Ammann, B., Andersen, S., Anderson, R., Andrič, M., Balakauskas, L., Barnekow, L., Batalova, V., Bergman, J., Birks, H., Björkman, L., Bjune, A., Borisova, O., Broothaerts, N., Carrion, J., Caseldine, C., Christiansen, J., Cui, Q., Currás, A., Czerwiński, S., David, R., Davies, A., De Jong, R., Di Rita, F., Dietre, B., Dörfler, W., Doyen, E., Edwards, K., Ejarque, A., Endtmann, E., Etienne, D., Faure, E., Feeser, I., Feurdean, A., Fischer, E., Fletcher, W., Franco-Múgica, F., Fredh, E., Froyd, C., Garcés-Pastor, S., García-Moreiras, I., Gauthier, E., Gil-Romera, G., González-Sampériz, P., Grant, M., Grindean, R., Haas, J., Hannon, G., Heather, A.-J., Heikkilä, M., Hjelle, K., Jahns, S., Jasiunas, N., Jiménez-Moreno, G., Jouffroy-Bapicot, I., Kabailienė, M., Kamerling, I., Kangur, M., Karpińska-Kołaczek, M., Kasianova, A., Kołaczek, P., Lagerås, P., Latalowa, M., Lechterbeck, J., Leroyer, C., Leydet, M., Lindbladh, M., Lisitsyna, O., López-Sáez, J.-A., Lowe, J., Luelmo-Lautenschlaeger, R., Lukanina, E., Macijauskaitė, L., Magri, D., Marguerie, D., Marquer, L., Martinez-Cortizas, A., Mehl, I., Mesa-Fernández, J., Mighall, T., Miola, A., Miras, Y., Morales-Molino, C., et al.: Testing the Effect of Relative Pollen Productivity on the REVEALS Model: A Validated Reconstruction of Europe-Wide Holocene Vegetation, Land (Basel), 12, 986, https://doi.org/10.3390/land12050986, 2023.

Simas, A. B., Barreto-Souza, W., and Rocha, A. V.: Improved estimators for a general class of beta regression models, Comput. Stat. Data Anal., 54, 348–366, https://doi.org/10.1016/j.csda.2009.08.017, 2010.

Staal, A., Tuinenburg, O. A., Bosmans, J. H. C., Holmgren, M., van Nes, E. H., Scheffer, M., Zemp, D. C., and Dekker, S. C.: Forest-rainfall cascades buffer against drought across the Amazon, Nat. Clim. Change, 8, 539–543, https://doi.org/10.1038/s41558-018-0177-y, 2018.

https://doi.org/10.5194/egusphere-2024-1523
Preprint. Discussion started: 27 May 2024

Sugita, S.: A Model of Pollen Source Area for an Entire Lake Surface, Quat. Res., 39, 239–244, https://doi.org/10.1006/qres.1993.1027, 1993.

Sugita, S.: Theory of quantitative reconstruction of vegetation I: Pollen from large sites REVEALS regional vegetation composition, Holocene, https://doi.org/10.1177/0959683607075837, 2007a.

Sugita, S.: Theory of quantitative reconstruction of vegetation II: all you need is LOVE, Holocene, 17, 243–257, https://doi.org/10.1177/0959683607075838, 2007b.

Trondman, A. -K., Gaillard, M. -J., Mazier, F., Sugita, S., Fyfe, R. M., Nielsen, A. B., Twiddle, C., Barratt, P., Birks, H. J. B., Bjune, A. E., Björkman, L., Broström, A., Caseldine, C., David, R., Dodson, J., Dörfler, W., Fischer, E., Geel, B., Giesecke, T., Hultberg, T., Kalnina, L., Kangur, M., Knaap, P., Koff, T., Kuneš, P., Lagerås, P., Latałowa, M., Lechterbeck, J., Leroyer, C., Leydet, M., Lindbladh, M., Marquer, L., Mitchell, F. J. G., Odgaard, B. V., Peglar, S. M., Persson, T., Poska, A., Rösch, M., Seppä, H., Veski, S., and Wick, L.: Pollen-based quantitative reconstructions of Holocene regional vegetation cover (plant-functional types and land-cover types) in Europe suitable for climate modelling, Glob. Chang. Biol., 21, 676–697, https://doi.org/10.1111/gcb.12737, 2015.

Turubanova, S., Potapov, P., Hansen, M. C., Li, X., Tyukavina, A., Pickens, A. H., Hernandez-Serna, A., Arranz, A. P., Guerra-Hernandez, J., Senf, C., Häme, T., Valbuena, R., Eklundh, L., Brovkina, O., Navrátilová, B., Novotný, J., Harris, N., and Stolle, F.: Tree canopy extent and height change in Europe, 2001–2021, quantified using Landsat data archive, Remote Sens. Environ., 298, 113797, https://doi.org/10.1016/j.rse.2023.113797, 2023.

Viedma, O., Moity, N., and Moreno, J. M.: Changes in landscape fire-hazard during the second half of the 20th century: Agriculture abandonment and the changing role of driving factors, Agric. Ecosyst. Environ., 207, 126–140, https://doi.org/10.1016/j.agee.2015.04.011, 2015.

Villegas-Diaz, R. and Harrison, S.P.: The SPECIAL Modern Pollen Data Set for Climate Reconstructions, version 2 (SMPDSv2). University of Reading. Dataset. https://doi.org/10.17864/1947.000389, 2022

Wei, D., González-Sampériz, P., Gil-Romera, G., Harrison, S. P., and Prentice, I. C.: Seasonal temperature and moisture changes in interior semi-arid Spain from the last interglacial to the Late Holocene, Quat. Res., 101, 143–155, https://doi.org/10.1017/qua.2020.108, 2021.

Weiss, H., Courty, M.-A., Wetterstrom, W., Guichard, F., Senior, L., Meadow, R., and Curnow, A.: The Genesis and Collapse of Third Millennium North Mesopotamian Civilization, Science, 261, 995–1004, https://doi.org/10.1126/science.261.5124.995, 1993.

Wörl, V., Jetschni, J., and Jochner-Oette, S.: Birch Pollen Deposition and Transport along an Altitudinal Gradient in the Bavarian Alps—A Case Study Using Gravimetric Pollen Traps in the Pollen Season 2020, Atmosphere, 13, 2007, https://doi.org/10.3390/atmos13122007, 2022.

Zanon, M., Davis, B. A. S., Marquer, L., Brewer, S., and Kaplan, J. O.: European forest cover during the past 12,000 years: A palynological reconstruction based on modern analogs and remote sensing, Front. Plant Sci., 9, 1–25, https://doi.org/10.3389/fpls.2018.00253, 2018.

https://doi.org/10.5194/egusphere-2024-1523
Preprint. Discussion started: 27 May 2024

Zapolska, A., Serge, M. A., Mazier, F., Quiquet, A., Renssen, H., Vrac, M., Fyfe, R., and Roche, D. M.: More than agriculture: Analysing time-cumulative human impact on European land-cover of second half of the Holocene, Quat. Sci. Rev., 314, 108227, https://doi.org/10.1016/j.quascirev.2023.108227, 2023.

Zhang, Y., Renssen, H., and Seppä, H.: Effects of melting ice sheets and orbital forcing on the early Holocene warming in the extratropical Northern Hemisphere, Clim. Past, 12, 1119–1135, https://doi.org/10.5194/cp-12-1119-2016, 2016.

Zhang, Y., Renssen, H., Seppä, H., and Valdes, P. J.: Holocene temperature trends in the extratropical Northern Hemisphere based on inter-model comparisons, J. Quat. Sci., 33, 464–476, https://doi.org/10.1002/jqs.3027, 2018.